Conformational Flexibility of Metalloporphyrin Skeletons As Studied by Racemization Profiles of Chiral *meso*-Substituted Metalloporphyrins with Molecular Asymmetry

Katsuaki Konishi, Yoshiki Mori, Takuzo Aida,* and Shohei Inoue†

Department of Chemistry and Biotechnology, Faculty of Engineering, University of Tokyo, Hongo, Bunkyo-ku, Tokyo 113, Japan

Received October 7, 1994

Introduction

Since the discovery of strained structures for the tetrapyrrole macrocycles in hemoproteins,[1] vitamin B_{12},[2] methylreductase,[3] and antenna chlorophylls,[4] interest in the synthesis and functions of nonplanar metalloporphyrins has emerged. Examples include metal complexes of *N*-substituted porphyrins, tightly strapped porphyrins,[5] *meso*-substituted octaalkylporphyrins,[6] and fully substituted porphyrins.[7] In addition to the substituents on the porphyrin ring, the central metal atom of a particular type possibly induces ruffling of the porphyrin skeleton, as exemplified by Ni(II)[8] and Pb(II)[9] octaethylporphyrins.

We have recently found that zinc *meso*-pivalamidoetioporphyrin I (**3b**) (Chart 1) undergoes thermal- and photo-induced conformational motion of the porphyrin skeleton in solution.[10] This observation takes advantage of the chirality of **3a**, originating from the enantiotopic structure of the precursor etioporphyrin I (**1**).[11] The pivalamide substituent at the *meso* position of **3a** is situated on either side of the enantiotopic porphyrin faces due to the steric repulsion with the neighboring pyrrole-β substituents, and **3a** is therefore chiral. Successful resolution of the antipodes of **3b** by chiral HPLC allowed us to study the conformational motion of the porphyrin skeleton by monitoring the racemization process.

Herein we report the synthesis and optical resolution of various chiral, *meso*-amido- and *meso*-alkenylporphyrins and their zinc, copper, and nickel complexes, and the flexibility of the metalloporphyrin skeletons is discussed on the basis of their racemization profiles.

Chart 1

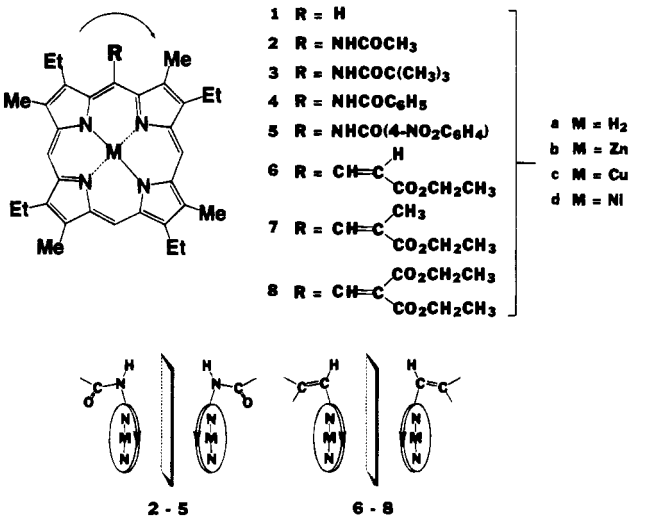

Results and Discussion

The *meso*-amido-[10] and *meso*-alkenylporphyrins[12,13] (**2a-8a**) were synthesized from 5-amino- and 5-formyletioporphyrins I, respectively. By using chiral HPLC, the antipodes of the free bases (**7a**, **8a**) and the zinc (**2b-5b**, **7b**) and copper complexes (**3c**, **7c**) were obtained in nearly optically pure forms. For example, **7b** showed two elution peaks (first fraction, **7b**-[F1]; second fraction, **7b**-[F2]) with hexane/EtOH (90/10 v/v) as eluent. The antipodes of **7b**, thus isolated, provided perfect mirror-image circular dichroism (CD) spectra of each other, where **7b**-[F1] showed a positive CD band in the Soret region, while **7b**-[F2] showed a negative one (Figure 1). On the other hand, the free-base amidoporphyrins (**2a-5a**) were only partially resolved (~60% enantiomeric excess) due to possible racemization in the HPLC column.[14,15] In contrast to the above examples, the antipodes of **6a-d**, which bear monosubstituted β-vinylic carbon atoms, were not resolved under similar HPLC conditions. HPLC resolutions of the nickel complexes (**3d**, **7d**, **8d**) were all unsuccessful, but the optically active nickel complex (**7d**) (Figure 1) could be obtained from the reaction of an antipode of **7a** (**7a**-[F1]) with $Ni(OAc)_2$ at 60 °C in $CHCl_3$/MeOH for 10 min.

† Present address: Department of Industrial Chemistry, Faculty of Engineering, Science University of Tokyo, Kagurazaka, Shinjuku-ku Tokyo 162, Japan.

(1) (a) Takano, T. *J. Mol. Biol.* **1977**, *110*, 537. (b) Deatherage, J. F.; Loe, R. S.; Anderson, C. M.; Moffat, K. *J. Mol.* Biol. **1976**, *104*, 687.
(2) (a) Glusker, J. In B_{12}; Dolphin, D., Ed.; Wiley: New York, 1982; Vol. 1, p 373. (b) Geno, M. K.; Halpern, J. *J. Am. Chem. Soc.* **1987**, *109*, 1238.
(3) (a) Furenlid, L. R.; Renner, M. W.; Fajer, J. *J. Am. Chem. Soc.* **1990**, *112*, 8987. (b) Furenlid, L. R.; Renner, M. W.; Fajer, J.; Smith, K. M. *J. Am. Chem. Soc.* **1990**, *112*, 1634. (c) Eshenmoser, A. *Ann. N.Y. Acad. Sci.* **1986**, *471*, 108.
(4) (a) Deisenhofer, J.; Michel, H. *Science* **1989**, *245*, 1463. (b) Tronrud, D. E.; Schmid, M. F.; Matthews, B. W. *J. Mol. Biol.* **1986**, *188*, 433. (c) Deisenhofer, J.; Epp, O.; Miki, K.; Huber, R.; Michel, H. *Nature* **1985**, *318*, 618. (d) Horning, T. L.; Fujita, E.; Fajer, J. *J. Am. Chem. Soc.* **1986**, *108*, 323. (e) Barkigia, K. M.; Chantraupong, L.; Smith, K. M. *J. Am. Chem. Soc.* **1988**, *110*, 7566.
(5) (a) Morgan, B.; Dolphin, D.; Jones, R. H.; Jones, T.; Einstein, F. W. B. *J. Org. Chem.* **1987**, *52*, 4628. (b) Simonis, U.; Walker, F. A.; Lee, P. L.; Hanquet, B. J.; Meyerhoff, D. J.; Scheidt, W. R. *J. Am. Chem. Soc.* **1987**, *109*, 2659.
(6) Hursthouse, M. B.; Neidle, S. *J. Chem. Soc., Chem. Commun.* **1972**, 449.
(7) (a) Sparks, L. D.; Medfroth, C. J.; Oark, M. S.; Chamberlain, J. R.; Ondrias, M. R.; Senge, M. O.; Smith, K. M.; Shelnutt, J. A. *J. Am. Chem. Soc.* **1993**, *115*, 581. (b) Medforth, C. J.; Senge, M. O.; Smith, K. M.; Sparks, L. D.; Shelnutt, J. A. *J. Am. Chem. Soc.* **1992**, *114*, 9859.
(8) (a) Cullen, D. L.; Meyer, E. F., Jr. *J. Am. Chem. Soc.* **1974**, *96*, 2095. (b) Brennan, T. D.; Scheidt, W. R.; Shelnutt, J. A. *J. Am. Chem. Soc.* **1988**, *110*, 3919.
(9) Barkigia, K. M.; Fajer, J.; Alder, A. D.; Williams, G. H. B. *Inorg. Chem.* **1980**, *19*, 2057.
(10) Konishi, K.; Miyazaki, K.; Aida, T.; Inoue, S. *J. Am. Chem. Soc.* **1990**, *112*, 5639.
(11) Examples of chiral porphyrins derived from enantiotopic porphyrins: (a) Kubo, H.; Aida, T.; Inoue, S.; Okamoto, Y. *J. Chem. Soc., Chem. Commun.* **1988**, 1015. (b) Konishi, K.; Sugino, T.; Aida, T.; Inoue, S. *J. Am. Chem. Soc.* **1991**, *113*, 6487. (c) Konishi, K.; Takahata, Y.; Aida, T.; Inoue, S.; Kuroda, R. *J. Am. Chem. Soc.* **1993**, *115*, 1169. (d) Konishi, K.; Oda, K.; Nishida, K.; Aida, T.; Inoue, S. *J. Am. Chem. Soc.* **1992**, *114*, 1313. (e) Chiang, L.-c.; Konishi, K.; Aida, T.; Inoue, S. *J. Chem. Soc., Chem. Commun.* **1992**, 254. (f) Konishi, K.; Yahara, K.; Toshishige, H.; Aida, T.; Inoue, S. *J. Am. Chem. Soc.* **1994**, *116*, 1337.
(12) Callot, H. J. *Bull. Soc. Chim. Fr.* **1973**, 3416.
(13) Witte, L.; Fuhrhop, J. H. *Angew. Chem., Int. Ed. Engl.* **1975**, *14*, 361.
(14) HPLC analysis showed two peaks with significant tailing and leading in between.
(15) When the eluate was kept at −78 °C, no further racemization was observed.

0020-1669/95/1334-1292$09.00/0

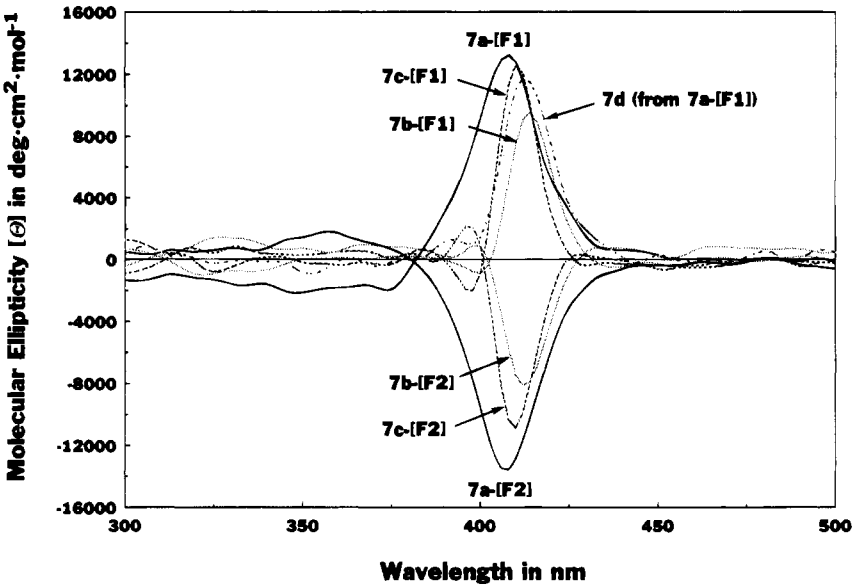

Figure 1. CD spectra of the antipodes of **7a-c** and **7d** (derived from **7a**-[F1]) in $CHCl_3$ at 25 °C.

Table 1. Rate Constants and Activation Parameters for the Thermal Racemization of Chiral *meso*-Substituted Porphyrins and Complexes[a]

compd	T (°C)	10^5k (s^{-1})	$\Delta G^{\ddagger}$ [b] (kcal·mol^{-1})	$\Delta S^{\ddagger}$ [b] (eu)	$\Delta H^{\ddagger}$ [b] (kcal·mol^{-1})
2b[c]	40	3.1	nd	nd	nd
3b[c]	28.5	2.1	24.1	18	29.4
	40	12	23.9		
3c[c]	22	48	21.7	3	22.5
	28.5	140	21.7		
4b[c]	28.5	0.58	24.8	5	26.4
	40	4.6	24.7		
5b[c]	40	4.5	nd	nd	nd
7a[d]	60	5.9	25.9	−9	23.1
	70	15	26.0		
7b[d]	60	1.7	26.6	−1	26.3
	70	6.9	26.6		
7c[d]	60	3.0	26.0	2	26.6
	70	14	26.0		
7d[d,e]	70	32	nd	nd	nd
8d[d]	60	7.5	25.9	−6	23.9
	70	19	26.0		

[a] From changes in enantiomeric excess monitored by chiral HPLC. [b] From rate constants at three different temperatures. [c] In hexane/EtOH/$CHCl_3$ (70/20/10 v/v, $(1.8-2.0) \times 10^{-4}$ M). [d] In xylene ($(0.8-1.2) \times 10^{-4}$ M). [e] From changes in enantiomeric excess monitored by CD (see ref 16).

The alkenyl- and amidoporphyrin families both racemized thermally. The rate constants and activation parameters for the thermal racemization of the selected antipodes are summarized in Table 1,[16] which clearly indicates that the alkenylporphyrin family is more reluctant to racemize than the amidoporphyrin family. Typically, at 40 °C in hexane/EtOH/$CHCl_3$ (70/20/10 in v/v), the zinc alkenylporphyrin (**7b**-[F1], 1.0×10^{-4} M) hardly racemized (●) (Figure 2), whereas the pivalamido-substituted analogue (**3b**-[F1]) racemized to 67 and 34% enantiomeric excess in only 25 and 60 min, respectively (□). As for the effect of the central metal atom, the zinc complexes (**3b**, **7b**) were evidently more reluctant to racemize than the copper complexes (**3c**, **7c**), while the free bases (**3a**,[10] **7a**) were much easier to racemize. Among the alkenylporphyrin family (**7a-d**), the nickel complex (**7d**) racemized the most rapidly: At 70 °C in xylene, **7d** (derived from **7a**-[F1]) racemized at a rate constant of 3.2×10^{-4} s^{-1}, which is more than twice as high as that of the free base (**7a**) (Table 1). Thus, the conformational flexibility of the metalloporphyrin skeleton increases in the order Zn < Cu < free base < Ni.[17]

Among the four zinc amidoporphyrin complexes (**2b-5b**), the antipode having a pivalamido substituent (**3b**) racemized more easily than the other (Table 1), possibly due to the strained porphyrin skeleton induced by the bulky *tert*-butyl group. As for the alkenylporphyrin family, $\Delta G^{\ddagger}$ values for **7a** and **8a** are comparable to each other, indicating that the β-substituent at the alkenyl group does not affect the conformational restriction of the porphyrin skeleton.

Another interesting observation is the base-promoted racemization observed for the zinc complexes: At 60 °C, the zinc alkenylporphyrin (**7b**-[F1], 1.0×10^{-4} M) racemized more rapidly in xylene containing 1% pyridine (☆, $k = 3.7 \times 10^{-5}$ s^{-1}) than in xylene alone (○, $k = 1.7 \times 10^{-5}$ s^{-1}) (Figure 2). A similar trend was observed for the zinc pivalamidoporphyrin complex, where **3b**-[F1] in hexane/EtOH/$CHCl_3$ (70/20/10 v/v) containing 1% pyridine racemized even at a low temperature such as 20 °C (◩), whereas no appreciable racemization took place in the absence of pyridine under otherwise the same conditions (■) (Figure 2). X-ray crystallographic studies have shown that the structure of zinc porphyrin, upon axial coordination of a base, changes from a square-planar[18] to square-pyramidal conformation.[19] Thus, the base-promoted racemization in Figure 2 is considered to be due to the ring strain of the square-pyramidal zinc porphyrin complex having a pyridine ligand.[20] Consistently, such a base-accelerated racemization was not observed for the copper complex (**7c**) having no coordination ability.

(16) Racemization profiles of *e.g.*, **7**, as observed by chiral HPLC and CD spectroscopy, were virtually identical to each other.

(17) For atropisomerization of 5,10,15,20-tetrakis(2′-amidophenyl)porphines and the metal complexes, the rate has been reported to increase in the same order (Zn < Cu < free base < Ni): (a) Freitag, R. A.; Mercer-Smith, J. A.; Whitten, D. G. *J. Am. Chem. Soc.* **1981**, *103*, 1226. (b) Freitag, R. A.; Whitten, D. G. *J. Phys. Chem.* **1983**, *87*, 3918.

(18) (a) Scheidt, W. R.; Mondal, J. U.; Eigenbrot, C. W.; Adler, A. D.; Radonovich, L. J.; Hoard, J. L. *Inorg. Chem.* **1986**, *25*, 795. (b) Scheidt, W. R.; Kastner, M. E.; Hatano, K. *Inorg. Chem.* **1978**, *17*, 706.

(19) (a) Collins, D. M.; Hoard, J. L. *J. Am. Chem. Soc.* **1970**, *92*, 3761. (b) Bobrik, M. A.; Walker, F. A. *Inorg. Chem.* **1980**, *19*, 3383. (c) Cullen, D. L.; Meyer, E. F. *Acta Crystallogr.* **1976**, *B32*, 2259.

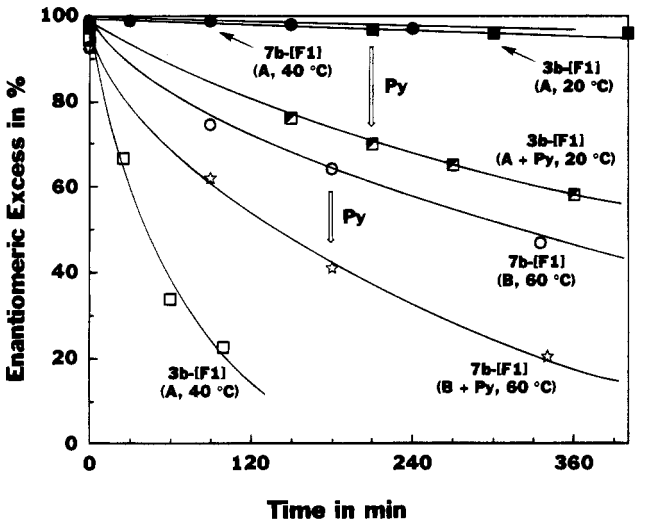

Figure 2. Racemization profiles of **3b**-[F1] and **7b**-[F1] in hexane/EtOH/$CHCl_3$ (70/20/10 v/v) (A), hexane/EtOH/$CHCl_3$/pyridine (70/20/10/1 v/v) (A + Py), xylene (B), and xylene/pyridine (100/1 v/v) (B + Py) at 20, 40, and 60 °C.

As already described, irradiation of the zinc pivalamidoporphyrin (**3b**) with visible light (λ > 380 nm, xenon arc light) results in accelerated racemization.[10] However, this was not the case for the zinc alkenylporphyrin (**7b**).

In conclusion, several factors affecting the flexibility and conformational motion of the porphyrin skeleton were clarified through studies on the racemization profiles of the chiral *meso*-substituted porphyrin derivatives.

Experimental Section

Materials. Etioporphyrin I was synthesized from *tert*-butyl 4-ethyl-3,5-dimethylpyrrole-2-carboxylate.[21] 5-Aminoetioporphyrin I was prepared by nitration of etioporphyrin I with fuming HNO_3 followed by reduction with $SnCl_2$/HCl.[22] 5-Formyletioporphyrin I was obtained by the Vilsmeier formylation of copper etioporphyrin I followed by demetalation with concentrated H_2SO_4.[23] *meso*-Amidoetioporphyrins I and their metal complexes (**2**, **4**, **5**) were prepared similarly to the preparation of **3**.[10] *meso*-Alkenyletioporphyrins I (**6a**-**8a**) were synthesized from 5-formyletioporphyrin I by the Wittig reaction with phosphoranes for **6a** and **7a**[12] and the Knoevenagel reaction with diethyl malonate for **8a**.[13] The alkenyl substituents in **6a** and **7a** were found to take (*E*)-geometry, as determined by comparison of the ^{1}H NMR data with those for the octaethylporphyrin analogues.[12] The zinc, copper, and nickel complexes of **6**-**8** were prepared by using the metal acetate method[24] and characterized by UV−vis and silica gel TLC.

6a. UV−vis: λ_{max} (log ϵ) 626 nm (3.18), 578 (3.35), 538 (3.56), 500 (3.92), 403 (5.00). ^{1}H NMR: δ 10.35 (d, 1H, J = 16 Hz), 10.11 (s, 2H), 9.96 (s, 1H), 6.27 (d, 1H, J = 16 Hz), 4.54 (q, 2H), 4.10−3.95 (m, 8H), 3.65, 3.63, 3.61, 3.42 (s × 4, 12H), 3.62 (s, 3H), 3.42 (s, 3H), 1.93−1.81 (m, 9H), 1.52 (t, 3H), −3.22 (br, 2H).

7a. FAB-HRMS for $C_{38}H_{47}N_4O_2$ (MH^+): calcd m/z 591.3699; obsd m/z 591.3675. UV−vis: λ_{max} (log ϵ) 625 nm (3.12), 574 (3.53), 538 (3.56), 503 (3.90), 405 (4.99). ^{1}H NMR: δ 10.13 (s, 3H), 9.96 (s, 1H), 4.63 (q, 2H), 4.10−3.97 (m, 8H), 3.66, 3.64, 3.62, 3.37 (s × 4, 12H), 1.93−1.81 (m, 9H), 1.66−1.58 (t, 6H), 1.24 (s, 3H), −3.23 (br, 2H).

7b. UV−vis: λ_{max} (log ϵ) 573 nm (4.16), 536.5 (4.19), 407.5 (5.15), 357.5 (4.41).

7c. UV−vis: λ_{max} (log ϵ) 567.5 nm (3.82), 532 (3.75), 405 (5.08), 328.5 (3.86).

7d. UV−vis: λ_{max} (log ϵ) 563.5 nm (4.09), 530 (3.96), 405.5 (5.04), 342.5 (4.25).

8a. FAB-HRMS for $C_{40}H_{49}N_4O_4$ (MH^+): calcd m/z 649.3753; obsd m/z 649.3773. UV−vis: λ_{max} (log ϵ) 627 nm (3.54), 572 (3.80), 537 (3.86), 503 (4.13), 406 (5.17). ^{1}H NMR: δ 10.48 (s, 1H), 10.13, 10.11, 10.00 (s × 3, 3H), 4.62 (q, 2H), 4.21−3.85 (m, 8H), 3.66, 3.65, 3.63, 3.43 (s × 4, 12H), 2.72 (m, 2H), 1.90 (m, 9H), 1.72 (t, 3H), 1.54 (m, 3H), −0.82 (t, 3H), −3.30 (s, 2H).

Procedures. Optical Resolution by Chiral HPLC. Optical resolution by HPLC was carried out at a flow rate of 1.0 mL·min^{-1} at room temperature by using a 4.6 × 250-mm column packed with silica gel coated with cellulose tris((3,5-dimethylphenyl)carbamate) as a chiral stationary phase (Daicel Chiralcel OD), and the eluates were collected in flasks wrapped in aluminum foil. For **2**-**5**, hexane/EtOH/$CHCl_3$ (70/20/10 v/v) was used as eluent, and the eluates collected were stored at −78 °C. Retention times were as follows. **2b**: **2b**-[F1], 13.8 min; **2b**-[F2], 31.6 min. **3a**: **3a**-[F1], 8.4 min; **3a**-[F2], 16.9 min. **3b**: **3b**-[F1], 11.6 min; **3b**-[F2], 37.3 min. **3c**: **3c**-[F1], 9.1 min; **3c**-[F2], 24.4 min. **4b**: **4b**-[F1], 9.6 min; **4b**-[F2], 17.5 min. **5b**: **5b**-[F1], 9.9 min; **5b**-[F2], 18.9 min. For **7** and **8**, hexane/EtOH (70/30 v/v) was used as eluent, where the eluates collected were evaporated to dryness at 20 °C under high vacuum and stored at 0 °C (enantiomeric excess > 95%). Retention times were as follows. **7a**: **7a**-[F1], 8.4 min; **7a**-[F2], 15.0 min. **7b**: **7b**-[F1], 5.5 min; **7b**-[F2], 9.7 min. **7c**: **7c**-[F1], 5.5 min; **7c**-[F2], 7.7 min. **8a**: **8a**-[F1], 10.0 min; **8a**-[F2], 15.8 min.

A solution of the antipode in a test tube (diameter 10 mm) was thermostated at a designated temperature, and the change in the enantiomeric excess was monitored by chiral HPLC or CD spectroscopy.

Measurements. Absorption and circular dichroism (CD) spectra were recorded in $CHCl_3$ at 25 °C on a JASCO Type U-best 50 spectrometer and a Jasco Type-J-720 spectropolarimeter, respectively. ^{1}H NMR spectra were recorded in $CDCl_3$ at 25 °C on a JEOL Type GSX-270 spectrometer operating at 270 MHz. Chemical shifts (ppm) were determined with respect to $CHCl_3$ (δ 7.28) as internal standard. FAB-MS spectra were recorded on a JEOL JMS-HX110 spectrometer using a 3-nitrobenzyl alcohol matrix.

Acknowledgment. We thank Dr. N. Morisaki of the Institute of Molecular and Cellular Biosciences, University of Tokyo, for FAB-MS measurements.

IC941152W

(20) Coordination of pyridine to **3b** and **7b** was confirmed by UV−vis. **3b**: λ_{max} 580 nm, 543, 411 (hexane/EtOH/$CHCl_3$ (70/20/10 v/v)), 584, 547, 417 (hexane/EtOH, $CHCl_3$/pyridine (70/20/10/1 v/v)). **7b**: λ_{max} 573 nm, 536.5, 407.5, 357.5 (xylene), 578, 548, 420, 341 (xylene/pyridine (100/1 v/v)).

(21) Evans, B.; Smith, K. M. *Tetrahedron* **1977**, *32*, 629.

(22) (a) Bonnett, R.; Stephenson, G. F. *J. Org. Chem.* **1971**, *36*, 2791. (b) Johnson, A. W.; Oldfield, D. *J. Chem. Soc. C* **1966**, 794.

(23) Infoffen, H. H.; Fuhrhop, J.-H.; Voigt, H.; Brockman, H., Jr. *Liebigs Ann. Chem.* **1966**, *133*, 695.

(24) Buchler, J. W. In *Porphyrins and Metalloporphyrins*; Smith, K. M., Ed.; Elsevier: Amsterdam, 1975; Chapter 5.